

Mathematical Modelling of Ring Resonator based Devices

Bishnupada Das
Electronics and Communication Engineering
College Of Engineering and Management ,Kolaghat
Kolaghat , West Bengal 721171

Ashutosh Kumar Jha
Electronics and Communication Engineering
College Of Engineering and Management ,
Kolaghat
Kolaghat , West Bengal 721171

Abstract : The field of signal processing provides a host of mathematical tools, such as linear system theory and Fourier transforms, which are used extensively in optics for the description of diffraction, spatial filtering, and holography. Optical filters can also benefit from the research already done in signal processing. In this project, digital signal processing concepts coupled with Linear System Theory are applied to the design and analysis of optical filters and temperature sensing. In particular, digital signal processing provides a readily available mathematical framework, the Z-transform, for the design of complex optical filters and allied applications. The relationship between digital filters and its optical counterpart is explored, and a brief historical overview of optical waveguide filters is given. Previously, spectrum analysis was the main application for optical filters. Recently, the demand for optical filters is increasing rapidly because of the deployment of commercial dense wavelength division multiplexed (DWDM) optical communication systems. With low loss optical fibers and broadband optical amplifiers, WDM systems have the potential to harness a huge bandwidth, and optical filters are essential to realizing this goal. In addition to traditional designs such as band-pass filters, new applications have emerged such as the need for filters to perform gain equalization and dispersion compensation and applications for WDM systems. As envisaged in 7th semester, this work has eventually opened new avenues in the field of sensing and may embark in to new horizon in optical Computing

Keyword : ν : frequency , Δ : Refractive index difference , n : Refractive Index , c : velocity of light , k : coupling ratio C : through port coupling coefficient , S : Cross port coupling coefficient , γ : round trip loss , α : Average ring loss , Q : Quality factor, MRR : Micro-ring resonator , CROW : Coupled-resonator optical waveguides, DWDM : Dense wavelength division multiplexing , SOI : Silicon-on-insulator , CMOS : Complementary Metal oxide semiconductor, MZI : Mach–Zehnder interferometer , FSR : Free spectral range , FPI : Fabry–Perot interferometer , FIR : Finite impulse response , IIR : Infinite impulse response , AR : Autoregressive , LTI : Linear, time-invariant

1. Concept Of Optical Filter

1.1 Introduction

Optical filters are completely described by their frequency response, which specifies how the magnitude and phase of each frequency component of an incoming signal is modified by the filter. While there are many types of optical filters, this work addresses those that allow an arbitrary frequency response to be approximated over a frequency range of interest. For example, thin-film interference filters can approximate arbitrary functions. A

complete set of functions is needed to closely approximate an arbitrary function. A well-known set consists of the sinusoidal functions whose weighted sum yields a Fourier series approximation. The Fourier series can be written in terms of exponential functions with complex arguments as follows:

$$H(\nu) = \sum_{n=0}^N [c_n e^{-j(2\pi\nu n - \phi_n)}] \quad \text{----- (1.1)}$$

where $H(\nu)$ is the frequency response of the filter, N is the filter order, and the $c_n e^{j\phi_n}$ terms are the complex weighting coefficients.

A weighted sum is common to any basis function decomposition. An incoming signal is split into a number of parts that are individually weighted and then recombined [1].

1.2 Literature Review

Concept of optical ring resonator and bending loss dates back in 1969 with the research of E.A.J. Marcatili [2]. Recently with the advancement of light wave technology different shapes other than circular ring resonators have also drawn much attention. This includes rectangular, elliptical or many other irregular shapes. Shapes apart, based on coupling technique these ring architectures can be vertically or serially coupled. Different coupling techniques have their own advantages and disadvantages. Kokubun et al., [3] have presented a scheme of fabrication technology for vertically coupled microring resonator (MRR). Also, the coupling strength between ring and the bus waveguides can be controlled more precisely [4] in vertically coupled microring resonator. This precise coupling between bus and ring waveguides leads to high-Q micro-ring resonator.

Ring resonators are usually constructed with coupled-resonator optical waveguides (CROW) structures, which are chains of coupled resonators in which light propagates through evanescent-field coupling. This coupling may be between ring to ring or bus to ring. Series coupled CROW structures are commonly used as they have high transmission and are easy to fabricate. These series coupled ring resonator structures have been studied for optical filtering, as these devices have boxlike transmission profile and excellent interstitial mode suppression characteristics.

Material wise glass silica has a wide transparency window (from visible to infrared), low intrinsic loss, and is also compatible with fiber-optic technology. The material loss is limited to Rayleigh scattering, the mature fiber-optic technology that has minimized intrinsic loss around the infrared region due to water and OHcontaminants [4]. Although glass silica waveguide with moderate refractive index contrast (Δ %) is a convenient means of fabricating ring resonator, performance of such devices is not satisfactory as ultra-compact optical filter used in commercial DWDM systems. As the bending radius decreases bending loss increases exponentially [5], there must be a trade-off between the ring length and bend loss in the ring resonator structure.

Silicon-on-insulator substrates (SOI) have generated an immense interest for micro and nano-photonics fabrication recently. Due to its high index contrast, electromagnetic field confinement leads to a strong integration density. When fabricated using silicon-on-insulator (SOI) platforms [6-7], the micro-resonators exhibit a great potential to build space, power, and spectrally efficient on-chip photonic networks that could be well integrated with CMOS electronics.

1.3 Different type of Interferometers

The optical analog of optical ring resonator is found in interferometers. Interferometers come in two general classes, although there are many variations of each. The first class is simply illustrated by the Mach-Zehnder interferometer (MZI). An incoming signal is split equally into two paths. One path is delayed with respect to the other by a time $T = \Delta Ln/c$ where n is the refractive index of the paths, c is the velocity of light in vacuum, and ΔL is the path length difference. The effective group index is used for waveguide delay paths. The signals in the two paths are then recombined. A partially reflecting mirror indicated by the dashed line in Fig. 2.1(a), in Chapter 2 acts as a beam splitter and combiner.

A waveguide version with directional couplers for the splitter and combiner is shown in Fig.2.1(b) in Chapter 2. Each implementation has two outputs that are power complementary. Coherent interference at the combiner leads to a sinusoidal frequency response whose period is inversely proportional to the path length difference. Its Fourier series is given by,

$$H(\nu) = \frac{1}{2}[1 - e^{-i2\pi\nu T}] \quad (1.2)$$

The frequency is referenced to a center frequency and normalized to one period, called the free spectral range (FSR). Changing the splitting or combining ratios adjusts the coefficients in the Fourier series. The number of terms in the Fourier series is ν_0 increased by splitting the incoming signal into more paths. An N term series results when the light is split into N paths, with each path having a relative delay that is T longer than the previous path. The distinguishing feature of this general class of interferometers is that there are a finite number of delays and no recirculating (or feedback) delay paths. The interfering paths are always feeding

forward even though the interferometer may be folded such as with a Michelson interferometer. The signal processing term used to designate this filter type is moving average (MA) or finite impulse response (FIR) [9].

1.4 Basic Ideas of Ring Resonator

The second class of interferometers is illustrated by the Fabry–Perot interferometer (FPI). The FPI consists of a cavity surrounded by two partial reflectors that are parallel to each other. The frequency response results from interference of multiple reflections from the mirrors. The output is the infinite sum of delayed versions of the input signal weighted by the round-trip cavity transmission. The waveguide analog is a ring resonator with two directional couplers. There are two outputs: *Out1* corresponds to the transmission response of the FPI, and *Out2* corresponds to its reflection response. Filters with feedback paths are classified as autoregressive (AR) or infinite impulse response (IIR) filters in signal processing. When several stages are cascaded, the resulting transmission response is described by one over a Fourier series as follows:

$$FSR = \frac{1}{T} = \frac{c}{nL_u} \quad (1.3)$$

The optical path lengths are typically integer multiples of the smallest path length difference. The unit delay is defined as $T = \frac{c}{nL_u}$ where L_u is the smallest path length and is called the *unit delay length*. Digital signal processing techniques are relevant to optical filters because they are linear, time-invariant (LTI) systems that have discrete delays. In glass, with a refractive index of 1.5, a unit delay of 100 ps corresponds to a unit length of 2 cm. Because the delays are discrete values of the unit delay, the frequency response is periodic. One period is defined as the *FSR*, which is related to the *unit delay* and unit length as follows:

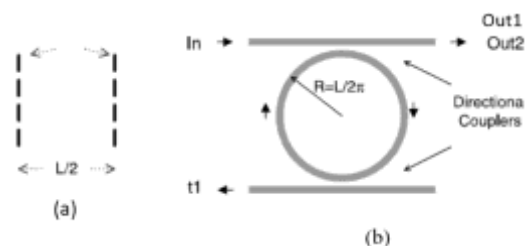
$$FSR = \frac{1}{T} = \frac{c}{nL_u}$$

The FSR of a filter with a 100 ps unit delay is 10 GHz. At 1550 nm, 10 GHz corresponds to $\Delta\lambda = 0.08$ nm. The shorter the unit delay, the larger the FSR.

Because several centimeters of fiber are needed for splicing, optical fiber filters can have very small FSRs (for example, $L_u = 50$ cm and $n = 1.5$ corresponds to a $FSR = 400$ MHz) compared to

several gigahertz (GHz) needed for separating high bit-rate communication channels [10].

2. Mathematical modeling of the ring resonator based Optical filter



resonator based Optical filter

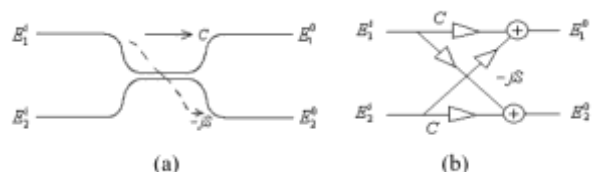
2.1 Transfer Matrix formulation and signal flow graph

The Fabry-Perot interferometer as discussed in Chapter–I consists of two partial reflectors that are parallel to each other as shown in Fig.2.1(a). The frequency response results from the interference of multiple reflections from mirrors.

Free spectral range (FSR) is the spacing between two resonant peaks. Wide

FSR is useful for multiplexing of communication channels. For this purpose, wide FSR and low crosstalk are required. Any filter, digital or optical can be represented as a linear time invariant (LTI) system. The optical path lengths are typically integer multiples of the smallest path length difference called unit delay length (L_u). The *unit delay* is defined as $T = nL_u/c$ where n is the refractive index and c is the velocity of the light. In *delay line signal processing* approach, a discrete signal is generally obtained by sampling a continuous signal at $t = NT$, where N is the sample number and T is the sampling interval. The mathematical relation between *unit delay* and *free spectral range (FSR)* is given by equation (1.3)[11].

Fig. 2.1(a) Mirror Splitter and combiner (b) Waveguide analog of a Fig. 2.1(a) shows the schematics of directional optical coupler which is a passive optical component without gain used for designing an optical filter. Fig.2.1 (b) shows the block diagram of the directional optical coupler. A single ring resonator with



evanescently side coupled to waveguides is shown in Fig.2.2(a) and the equivalent z-transform schematics (signal flow graph) of the same is shown in Fig. 2.2(b). When two optical waveguides are evanescently side coupled with each other the relationship between input and output can be expressed as a 2x2 transfer matrix as shown in equation (2.1).

Fig.2.2 (a) Coupling of evanescent fields in two adjacent waveguides (b) Equivalent signal flow diagram

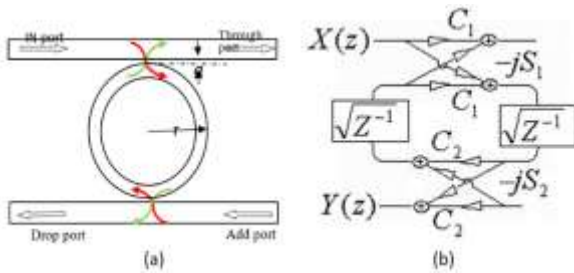


Fig.2.3(a): A single ring resonator (SRR) with evanescently side coupled to waveguides (b) Z transform equivalent of SRR.

$$\begin{bmatrix} E_1^0 \\ E_2^0 \end{bmatrix} = q \begin{bmatrix} C & -jS \\ -jS & C \end{bmatrix} \begin{bmatrix} E_1^i \\ E_2^i \end{bmatrix} \quad (2.1)$$

Here, E_1^i, E_2^i represent coupler input, E_1^o, E_2^o represents coupler outputs, q is the amplitude transmission coefficient of the coupler[12].

If κ is the power coupling ratio of the optical directional coupler, the through port transmission coefficient (C) as shown in Fig. 2.1(a) is represented by

$$C = \sqrt{1-\kappa} \quad (2.2)$$

and cross port transmission is given by

$$-jS = -j\sqrt{\kappa} \quad (2.3)$$

Using Mason's Rule, the overall transmittance of the signal flow graph (Fig.2.3b) is given by [12]

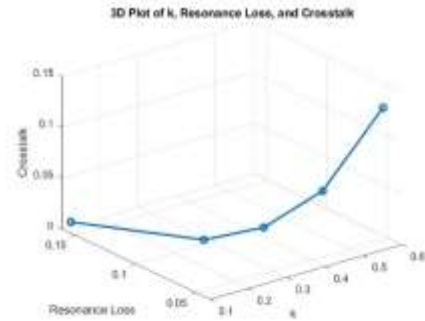
$$T_{f1}(z) = -\frac{S_1 S_2 \sqrt{\gamma z^{-1}}}{1 - C_1 C_2 \gamma z^{-1}} \quad (2.4)$$

In the expression (2.4) the round-trip loss $\gamma = \exp(-aL)$, where a is average ring loss per unit length and L is the ring perimeter. z^{-1} is generally known as *unit delay* in zdomain.

2.2 Simulation Results

2.2.1 When the waveguide material is glass silica SiO₂ with refractive index 1.46

Glass silica has a wide transparency window (from visible to infrared), Low intrinsic loss, and it is also compatible with fiber-optic technology. The material loss is limited to Rayleigh scattering. Mature fiber-optic technology that has minimized intrinsic loss around the infrared region due to water and OH⁻contaminants. Further there are convenient means of fabricating ring resonator. As the bending radius decreases bending loss increased exponentially, there must be a trade-off between the bending radius and bending loss for realization of practical devices.



In this work we have assumed a single ring resonator (SRR) with ring length of 1.0443cm, with round trip loss 0.9880dB. Transmission characteristics for different values of coupling coefficients are shown in the Fig2.4 below. From the figure it is evident that with the increasing value of coupling coefficients resonance loss decreases but crosstalk increases.

Variation of crosstalk and resonance loss with assumed coupling coefficients are shown in Fig. 2.5. Optimum result is obtained with $k_1=k_2=0.234$ for which obtainable FSR for such a system is 1.966 GHz.

Table I: Single Ring Resonator Data for Optimization (SiO₂)

Sl. No.	Coupling coefficient(k) $k_1=k_2=k$	FSR (GHz)	Resonance loss (%)	Cross talk (%)
1	0.123	1.966	16.10	0.42
2	0.234	1.966	8.60	1.72
3	0.315	1.966	6.20	3.42
4	0.418	1.966	4.60	6.80

5	0.550	1.966	3.80	14.2
---	-------	-------	------	------

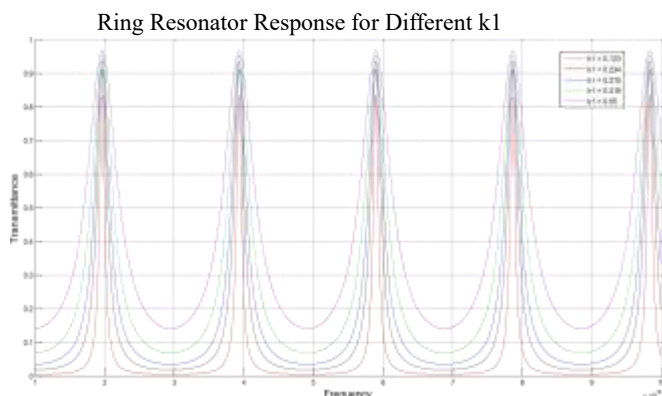


Fig. 2.4 Frequency response of single ring resonator made of SiO₂ with refractive index 1.46.

Table II: Single Ring Resonator Data for Optimization (SOI)

Sl.No	Coupling coefficient(k) $k_1=k_2=k$	FSR (GHz)	Resonance loss (%)	Cross talk (%)
1	0.123	1.683	1.63	0.42
2	0.234	1.683	8.50	1.72
3	0.315	1.683	6.16	3.42
4	0.418	1.683	4.49	6.8
5	0.55	1.683	3.10	14.2

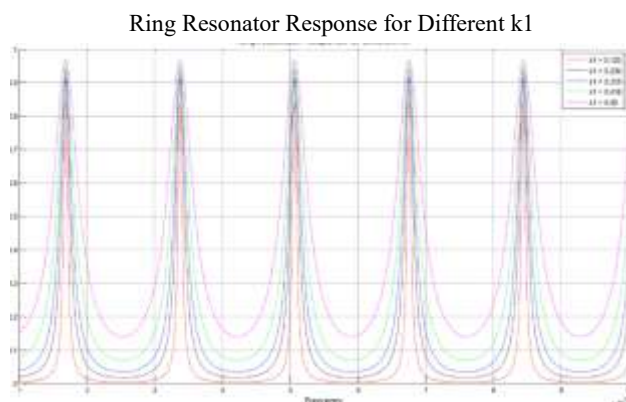


Fig.2. 6 Frequency response of single ring resonator made of SOI with RI 1.7.

Fig.2.5 Variation of crosstalk and resonance loss with coupling coefficients

2.2.2 When the waveguide material is SOI (n=1.7)

Due to its high index contrast in silicon-on-insulator (SOI) substrates electromagnetic field confinement leads to a strong integration density. Micro rings of much reduced diameter are possible, resulting in wider FSR. When fabricated using SOI platforms, micro resonators exhibit a greater compatibility to build space, power and spectrally efficient on-chip photonic networks that could be well integrated with CMOS electronics with reduced footprint. From the transmission characteristics curve given in the Fig. 2.6 it is evident that the optimum result obtained in this case for coupling coefficient $k_1=k_2=0.123$ with obtainable FSR 1.683 GHz. Although this FSR is little less than that obtained with SiO₂ ring resonator with the similar parameters, it gives much flexibility in system miniaturization with enhanced FSR and mitigated bending loss.

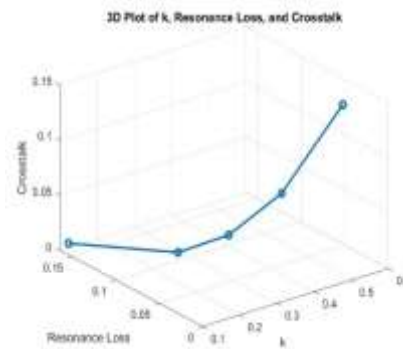


Fig.2.7 Variation of crosstalk and resonance loss with coupling coefficients for SOI single ring resonator (SRR)

3. Application of Optical Ring resonator as Temperature Sensor

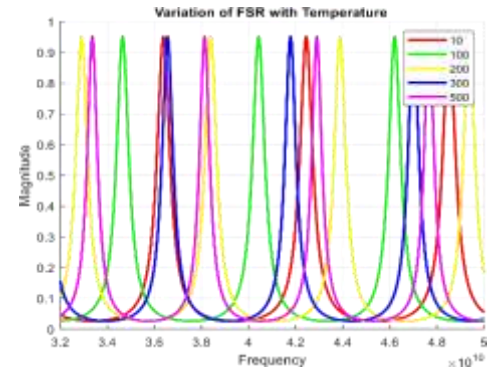
Optical sensor using micro-ring resonators made of silicon-based waveguides are enabling technology in the ever-expanding field of photonic sensors. Silicon photonics has attracted immense attention because of its advantages like ultra-small footprint and flexible integration with electronic integrated circuits. Due to its compactness, high sensitivity and selectivity, multi-channel sensing, compatibility with fiber optic cables and shorter response time researchers are gradually inclining towards photonic sensors.

Due to versatile compatibility, sensors based on Ring Resonators are gaining grounds and popularity over other sensing systems. Some of the smallest sensors (in nano-scale) are based on ring resonator [14]. Ring resonator provides high sensitivity and selectivity with a compact design and moreover fabrication can be done with much ease using existing fabrication processes like SOI. Ring resonators facilitates label free bio-sensing [15], gas and vapor sensing [16], physical parameters like speed, pressure [17], and *temperature sensing* [18] and even virus and cancer detection [19].

Temperature sensing plays a crucial role in modern life ranging from physiological monitoring, biological and medical application, environmental control, manufacturing and automobiles. But there is also a need to measure and monitor temperature in many complex electronic circuits. Electronic circuits such as motherboards in super-computers and other complex electronic chips are prone to high temperature change. The response of the processor as well as life of the components is highly dependent on the temperature rise. Furthermore, without proper control of the temperature the circuit might get burnt. So proper monitoring of temperature is crucial to enhance the performance of the circuit and also for protection of the circuit components from damaging due to overheating. The temperature rise in electronic circuits results due to atmospheric heat or heat generated by the circuit components.

3.1 Temperature Sensor

Temperature sensor based on optical ring resonator has been demonstrated with its constituent material as silicon (Si-fiber)



in this project. It has been done through optical delay line signal processing technique in Z-domain already discussed in earlier chapters. The group index of material varies with the change in temperature due to the thermo-optic effect in materials. Thus, temperature dependence of free spectral range (FSR) forms the basis of modeling the sensors. Silicon (Si) fiber based optical sensor can sense the temperature in the range 30–500⁰C. Obtainable temperature sensitivities for Si-fibers is 2.97 MHz/⁰C.

The temperature dependence of the ring resonator based optical sensor can be derived from the change of the group refractive index with the change in temperature [12] as shown in Eq. (8),

$$n_g = n_{ei}(f_0, T_0) + f_0 \frac{dn_{ei}}{df_{(f_0, T_0)}} = n_{ei}(\lambda_0, T_0) - \lambda_0 \frac{dn_{ei}}{d\lambda_{(\lambda_0, T_0)}} \quad (3.1)$$

where n_{ei} is the refractive index for a diffraction-based delay line or effective refractive index. f_0 and T_0 being it's center frequency and temperature respectively. It is evident from (8) that the group index depends on both the temperature and frequency. In this project we are utilizing both these attributes for developing an optical temperature sensor. The variation of the refractive index due to change in temperature for realizing a highly sensitive optical wide range sensor is the object of the project which has been designed in accordance with the recommended data provided by Li et al. [20]. The group index depends on the frequency component as well. Hence, with the change in the group index, free spectral range (FSR) of the

optical resonator also changes as shown in Eq. (9)

$$FSR = \frac{C}{n_{gr} L_u} \quad (3.2)$$

3.2 Computed Results

Simulation is carried out in MATLAB. The Silicon ring perimeter in this case has been assumed to be 1.446 cm, with coupling coefficients in a single ring resonator (SRR) $k_1=k_2=0.285$. Small ring radius will give a wide temperature sensing range due to its wider FSR. As temperature in an electronic circuit may exceed 80°C, a greater sensing range is one of our design priorities. We have found the resonance frequency or wavelength dependence with temperature and Figure 3.1 Fig 3.2 shows the shift in resonant peaks with temperature. In this project we have considered the

Fig.3.1 Shift in resonance peak with temperature

temperature from 10°C to 500°C and we have achieved a frequency shift of approximately 0.017GHz/°C rise with temperature.



Fig. 3.2 Variation of FSR with temperature in a Si single ring resonator

3.3 Conclusions and Discussions

Due to the nature of the optical ring resonator and how it filters certain wavelengths of light passing through, it is possible to create high-order optical filters by cascading many optical ring resonators in series. This would allow for "small size, low losses, and integrability into [existing] optical networks. Additionally, since the resonance wavelengths can be changed by simply increasing or

decreasing the radius of each ring, the filters can be considered tunable. This basic property can be used to create a sort of mechanical sensor. If an optical fiber experiences mechanical strain, the dimensions of the fiber will be altered, thus resulting in a change in the resonant wavelength of light emitted. This can be used to monitor fibers or waveguides for changes in their dimensions. The tuning process can be affected also by a change of refractive index using various means including thermo-optic, electro-optic or all optical effects.

Electro-optic and all-optical tuning are faster than thermal and mechanical means, and hence find various applications including in optical communication. Optical modulators with a high-Q micro-ring are reported to yield outstandingly small power of modulation at a speed of > 50 Gbit/s at cost of a tuning power to match wavelength of the light source. A ring modulator placed in a Fabry-Perot laser cavity was reported to eliminate the tuning power by automatic matching of the laser wavelength with that of the ring modulator while maintaining high-speed ultralow-power modulation of a Si micro ring modulator.

Temperature shifts the resonance spectra of ring resonator filters depending on the materials used for fabricating the device. The temperature induced effective index shift in a ring waveguide has been effectively utilized in designing a temperature sensor, which can measure temperature from 10°C to 500°C. It was observed that FSR changes inversely with the temperature.

Optical temperature sensors are very useful in those applications that demand distributed measurement in harsh environment. These optical sensors can be assembled for measuring temperature with high precision in oily environment like in gearboxes. They are also useful for sensing temperature in the fields of down-hole monitoring and civil structures.

3.4 Scope of Future works

Optical ring, cylindrical, and spherical resonators have also been proven useful in the field of biosensing, and a crucial research focus is the enhancement of biosensing performance. One of the main benefits of using ring resonators in biosensing is the small volume of sample specimen required

to obtain a given spectroscopy results in greatly reduced background Raman scattering and fluorescence signals from the solvent and other impurities. Resonators have also been used to characterize a variety of absorption spectra for the purposes of chemical identification, particularly in the gaseous phase.

Another potential application for optical ring resonators is in the form of whispering gallery mode switches. Micro disk lasers are stable and switch reliably and hence, are suitable as switching elements in all-optical networks. An all-optical switch based on a high-Quality factor (Q) cylindrical resonator has been proposed that allows for fast binary switching at low power.

Many researchers are interested in creating three-dimensional ring resonators with very high-quality factors. These dielectric spheres, also called microsphere resonators, were proposed as low-loss optical resonators with which to study cavity quantum electrodynamics with laser-cooled atoms or as ultrasensitive detectors for the detection of single trapped atoms.

Ring resonators have also proved useful as single photon sources for quantum information experiments. Many materials used to fabricate ring resonator circuits have non-linear responses to light at high enough intensities. This non-linearity allows for frequency modulation processes such as four-wave mixing and Spontaneous parametric down-conversion which generate photon pairs. Ring resonators amplify the efficiency of these processes as they allow the light to circulate around the ring.

4. Acknowledgments

We would like to express my sincere gratitude to our project guide Dr. Sabitabrata Dey, Prof-ECE, for providing his invaluable guidance, comments and suggestions throughout the course of the project. We are also grateful to the other faculty and staff members of the Department for extending their unconditional help, support and inspiration to complete this project'S.

5. References

- [1] J Dobrowolski, "Numerical methods for optical thin films," *Opt. & Photon. News*, pp. 25–33, 1997.
- [2] Marcatili, E.A.J., "Bends in Optical Dielectric Guides", *Bell System Technical Journal*, Vol 48, No. 7, Sept, 1969,pp 2103-2132.
- [3] Y. Kokubun, Y. Hatakeyama, M. Ogata, S. Suzuki and N. Zaizen, "Fabrication Technologies for Vertically Coupled Microring Resonator with Multilevel Crossing Busline and Ultracompact-Ring Radius", *IEEE J. of Selected Topics in Quantum Electronics*, Vol , No 1, January/February 2005.
- [4] Landobasa Y.M. Tobing and Pieter Dumon, "Fundamental Principles of Operation and Notes on Fabrication of Photonic Microresonators", *Photonic Microring Research and Application*, Springer-156(2010), chap-1.
- [5] Payam Rabiei, William H. Steier, Cheng Zhang, and Larry R. Dalton, "Polymer Micro-Ring Filters and Modulators", *J. of Lightwave Technol*, Vol. 20, No. 11, Nov. 2002,pp 1968-1975.
- [6] M. Lipson, "Guiding, modulating, and emitting light on silicon: challenges and opportunities," *J. Lightw. Technol.*, vol. 23, no. 12, pp.4222–4238, Dec. 2005.
- [7] B. Jalali, M. Paniccia, and G. Reed, "Silicon photonics," *IEEE Microw.Mag.*, vol. 7, no. 3, pp. 58–68, Jun. 2006.
- [8] R. Soref, "The past, present, and future of silicon photonics," *IEEE J. Sel. Topics Quantum Electron.*, vol. 12, no. 6, pp. 1678–1687, Nov./Dec. 2006.
- [9] B. Moslehi, J. Goodman, M. Tur, and H. Shaw, "Fiber-Optic Lattice Signal Processing," *Proc. IEEE*, vol. 72, no. 7, pp. 909–930, 1984
- [10] H. Kogelnik, "Filter Response of Nonuniform Almost-Periodic Structures," *Bell System Techn. J.*, vol. 55, no. 1, pp. 109–126, 1976.
- [11] H. Macleod, *Thin-film Optical Filters*. New York: McGraw-Hill, 1989.

- [12] C. Madsen and J. Zhao, “A General Planar Waveguide Autoregressive Optical Filter,” *J. Lightw. Technol.*, vol. 14, no. 3, pp. 437–447, 1996
- [13] Mason, S. J., “feedback properties of signal flow graphs,” *Proc. IRF*, Vol. 44, no. 7, pp. 920–926, Jul 1956.
- [14] Z. Tian, S. S.-H. Yam, J. Barnes, W. Bock, P. Greig, J. M. Fraser, H.- P. Loock, and R. D. Oleschuk, “Refractive index sensing with mach– zehnder interferometer based on concatenating two single-mode fiber tapers,” *IEEE Photonics Technology Letters*, vol. 20, no. 8, pp. 626– 628, 2008.
- [15] M. Iqbal, M. A. Gleeson, B. Spaugh, F. Tybor, W. G. Gunn, M. Hochberg, T. Baehr Jones, R. C. Bailey, and L. C. Gunn, “Label-free biosensor arrays based on silicon ring resonators and high-speed optical scanning instrumentation,” *IEEE Journal of Selected Topics in Quantum Electronics*, vol. 16, no. 3, pp. 654–661, 2010.
- [16] N. A. Yebo, P. Lommens, Z. Hens, and R. Baets, “An integrated optic ethanol vapor sensor based on a silicon-on-insulator microring resonator coated with a porous zno film,” *Optics Express*, vol. 18, no. 11, pp. 11 859–11 866, 2010.
- [17] G. N. De Brabander, J. T. Boyd, and G. Beheim, “Integrated optical ring resonator with micromechanical diaphragms for pressure sensing,” *IEEE Photonics technology letters*, vol. 6, no. 5, pp. 671–673, 1994.
- [18] M.-S. Kwon and W. H. Steier, “Microring-resonator-based sensor measuring both the concentration and temperature of a solution,” *Optics express*, vol. 16, no. 13, pp. 9372–9377, 2008.
- [19] H. Zhu, I. M. White, J. D. Suter, M. Zourob, and X. Fan, “Opto-fluidic micro-ring resonator for sensitive label-free viral detection,” *Analyst*, vol. 133, no. 3, pp. 356–360, 2008.
- [20] Li, H. H. , Refractive index of silicon and germanium and its wavelength and temperature derivatives. *Journal of Physics*, 9(3), 561–658. 198